Nighttime Ionospheric D-region: Equatorial and Non-equatorial

Neil R. Thomson,[1] and Wayne M. McRae[2]

[1]Physics Department, University of Otago, P.O. Box 56, Dunedin, 9054, New Zealand

[2]Gravitec Instruments Pty Ltd., c/o School of Physics (MO13), University of Western Australia, 35 Sterling Highway, Perth, WA6009, Australia

Abstract

Nighttime ionospheric D-region parameters are found to be generally well-modeled by the traditional H' and β as used by Wait and by the US Navy in their Earth-ionosphere VLF radio waveguide programs. New comparisons with non-equatorial, mainly all-sea VLF path observations reported over several decades are shown to be consistent with the previously determined height H' ~ 85.0 km and sharpness β ~ 0.63 km^{-1}. These paths include NPM (Hawaii) to Washington DC, Omega Hawaii and NLK (Seattle) to Japan, NWC (N.W. Australia) to Madagascar and NBA (Panama) to Colorado. In marked contrast, transequatorial path observations (even when nearly all-sea) are found to be often not well-modeled: for example, for Omega Japan and JJI (Japan) to Dunedin, New Zealand, the observed amplitudes are markedly lower than those which would be expected from H' ~ 85.0 km and β ~ 0.63 km^{-1}, or any other realistic values of H' and β. Other transequatorial observations compared with modeling include NWC to Japan, Omega Hawaii to Dunedin, and NPM (Hawaii) to Dunedin. It is suggested that the effects of irregularities in the equatorial electrojet may extend down into the nighttime D-region and so account for the observed equatorial VLF perturbations through scattering or mode conversion.

1. Introduction

The D-region is the lowest altitude part of the Earth's ionosphere. Its bottom edge forms the upper boundary, or ceiling, of the Earth-ionosphere waveguide which is bounded below by the oceans and the ground. Very Low Frequency (VLF) radio waves (~2-40 kHz) travel over the Earth's surface in this waveguide; observations of their propagation characteristics result in one of the best probes available for measuring the D-region. During the middle of the day these VLF signals reflect mainly from heights in the range ~55-75 km, while at night, the electron densities are lower, and most of the reflection takes place in the range ~75-90 km. These (partial) reflections occur because the electron densities (and hence refractive indices) increase rapidly (in the space of a wavelength) with height in these ranges, typically from a few per cm^3 (or less) up to several hundred or more per cm^3. These electron densities are not readily measured by means other than VLF. Reflected amplitudes of higher frequency radio signals, such as those used in incoherent scatter radars, tend to be too small and so are masked by noise or interference. The air density at these heights is too high for satellites, causing too much drag. Rockets are expensive and transient; although some have given good results, there have generally been too few to cope with diurnal, seasonal and latitudinal changes. In particular, flights at night have been especially few, with very tenuous results.

Because VLF radio waves can penetrate some distance into seawater and, because they can be readily detected after propagating for many thousands of km, the world's major naval powers have built a number of powerful transmitters to communicate with their submarines. The phase and amplitude of the received signals provides a good measure, typically averaged over quite long distances, of the height and sharpness of the lower edge of the D-region. The US Naval Ocean Systems Center (NOSC), has developed computer programs (MODESRCH/MODEFNDR, LWPC - Long Wave Propagation Capability) which take the input path parameters, calculate appropriate full-wave reflection coefficients for the waveguide boundaries, and search for those modal angles which give a phase change of 2π across the guide, taking into account the curvature of the Earth [e.g. *Morfitt and Shellman,* 1976]. Further discussions of the NOSC waveguide programs and comparisons with experimental data can be found in *Bickel et al.* [1970], *Morfitt* [1977], *Ferguson* [1980], *Morfitt et al.* [1981], *Pappert and Hitney* [1988], *CCIR* [1990], *Thomson* [1993], *Ferguson* [1995], *Cummer et al.* [1998], *McRae and Thomson* [2000, 2004], *Thomson and Clilverd* [2001], *Thomson et al.* [2005], *Cheng et al.* [2006], and *Thomson et al.* [2007].

The NOSC programs can take arbitrary electron density versus height profiles supplied by the user to describe the D-region and thus the ceiling of the waveguide. However, from the point of view of accurately predicting (or explaining) VLF propagation parameters, this approach effectively involves too many variables to be manageable in our present state of knowledge of the D-region. As previously [*Thomson,* 1993; *McRae and Thomson,* 2000; *Thomson et al.* 2007], we follow the work of the NOSC group by characterizing the D-region with a Wait ionosphere defined by just two parameters, the 'reflection height', H', in km, and the exponential sharpness factor, β, in km^{-1} [*Wait and Spies,* 1964] giving the electron density (m^{-3}) as a function of height, z (km), as $N(z) = 1.43 \times 10^{13} \exp(-0.15H') \exp[(\beta - 0.15)(z - H')]$. The studies referenced in the previous paragraph also found this to be a satisfactory simplification. The LWPC version used here includes the modifications described by

McRae and Thomson [2000] to assure that LWPC uses a full range of modes and electron densities (as does MODEFNDR).

Daytime propagation is particularly stable, resulting in quite well-defined values of height, *H'*, and sharpness, β, characterizing the lower D-region, thus enabling reliable calculation of the received VLF amplitudes and phases [*Thomson,* 1993; *McRae and Thomson*, 2000]. VLF propagation at night is significantly more variable than by day. This makes it very desirable to take measurements over many nights and paths to establish a reliable pattern of average behavior. Even so, despite many observations and much modeling over several decades, consistent values of *H'* and β for nighttime have been slow to emerge.

NOSC (in LWPC), based on a relatively small number of aircraft flights, recommended H' = 87 km and β = 0.50 km^{-1} at night away from high latitudes. Recently, *Thomson et al*. [2007] found that, for *non-equatorial* nighttime paths, good agreement was found between their VLF observations and modeling, using H' = 85.1 ± 0.04 km and β = 0.63 ± 0.04 km^{-1}, for their six such long, nearly all-sea paths. (For five of these paths both phase and amplitude observations were matched; for the other path only amplitude was matched due to lack of phase observations.) They also noted that this agreement, while very good, did not seem to extend (at least consistently) to paths which were mainly over land or which, even if nearly all-sea, passed through the equatorial regions.

Here we compare nighttime VLF observations and modeling for several VLF *transequatorial* paths, some measured by ourselves and some by others, to ascertain the nature and extent of the disagreements. Before doing this we compare a number of *non-equatorial* observations, reported in the literature by others over the last few decades, with the modeling of *Thomson et al*. [2007]. We do this because *Thomson et* *al*. [2007] had a relatively modest number of non-equatorial observations available compared with the total VLF nighttime observations by others over both many years and many paths. The aim is to be sure that a good range of nighttime *non-equatorial* paths and frequencies are consistently modeled before determining the extent of any inconsistencies in the *transequatorial* cases.

Because daytime propagation is fairly predictable, and certainly more so than nighttime propagation, we mainly use the *differences* between day and night amplitudes and the *differences* between day and night phases as the basis for determining the nighttime ionospheric parameters. This avoids the difficulty that the radiated powers of many of the transmitters were not well-known at the times of the receiver measurements. This use of day-night differences removes the need for any accurate knowledge of either the transmitter's radiated power or transmitter's phase. However, in the case of the US Navy's own amplitude measurements at Washington DC reported by *Rhoads and Garner* [1967], and discussed in the next section, the relevant radiated powers are available and so can be taken into account.

For each frequency, on each VLF path, LWPC is thus used to calculate the expected received nighttime amplitudes and phases for a range of possible *H'* and β. The available observed amplitudes and phases for the path are then compared in appropriate plots to determine whether they are in satisfactory agreement with the values (85.1 km and 0.63 km^{-1}) previously determined by *Thomson et al.* [2007]. Details of the locations of the transmitters, receivers and paths used are given in Table 1 and Figure 1.

2. Non-equatorial Observations and Modeling

2.1 NPM, Hawaii, amplitudes at Washington, DC

Rhoads and Garner [1967], US Naval Research Laboratory, recorded absolute field strengths near Washington DC for signals on several VLF frequencies from NPM and from Haiku in Hawaii, 7.8 Mm away, for the two month period 13 May to 13 July 1965 (i.e. essentially summer, solar minimum). Their ground-based measurements are one of the few sets supported by near simultaneous measurements of transmitter radiated power (by measuring the antenna current). They were thus able to present their results in dB above 1 μV/m normalized for 1 kW radiated power (though, of course, the actual radiated power would have been much higher).

Figure 2 shows results from LWPC calculations for NPM on the four principal frequencies reported by *Rhoads and Garner* [1967] at Washington DC for various values of *H'* (in the range 83-87 km) and β (in the range 0.50-0.80 km^{-1}), appropriate for nighttime propagation. The amplitudes are from LWPC's standard output in dB above 1 μV/m (for a radiated power of 1 kW). The text box, near the bottom of each of these panels, shows the amplitudes calculated by LWPC for the appropriate panel frequency near *path mid-day* for the (summer) dates shown; these calculations are given for both solar minimum (using the daytime *H'* and β values determined by *McRae and Thomson,* [2000]) and solar maximum (using the daytime *H'* and β values determined by *Thomson,* [1993]). Also shown, in each text box, is the mean observed difference in amplitude between day and night from the measurements of *Rhoads and Garner* [1967, Table 2]. The daily scatter of their day-night differences about the mean day-night difference is ~ ±2.5 dB over a few tens of days; so the random error for each of the mean observed amplitude differences is ~ ±0.5 dB.

Table 2 below compares the daytime observed amplitudes at Washington DC with the LWPC-calculated solar minimum values (since 1965 was near solar minimum). Clearly the agreement is good. The average of these (closely agreeing) mid-day amplitudes at each frequency was then combined with the appropriate day-night observed difference to give the effective observed nighttime amplitude shown as thick bold horizontal straight lines in each panel of Figure 2. It can thus be seen, that *H'* = 85.1 km and β = 0.63 km^{-1} (the values found by *Thomson et al.*, [2007]) give good agreement between the observed nighttime amplitudes and modeling for this 7.8 Mm, part-land, part-sea path. No phase measurements were available for this path.

About half of this 7.8 Mm path, from NPM, Hawaii, to Washington DC, is over the Pacific Ocean and about half is over land (the continental USA). So, although the agreement in Table 2 between the daytime and calculated amplitudes is good to a few tenths of a dB, this is confirming the daytime model (which uses the *H'* and β values determined by *McRae and Thomson*, [2001]) only to ~2 dB because of uncertainties in the ground conductivity built into LWPC. To some extent this effect of uncertainty in the ground conductivity in LWPC is reduced for nighttime propagation by our using here the observed *difference* in the day-night VLF observations.

2.2 Omega, Hawaii, phases at Inubo, Japan.

Kikuchi [1983] recorded the diurnal phase changes over the 6.1 Mm all-sea path Omega, Haiku, Hawaii, to Inubo, Japan, on four frequencies, over intervals of 3-4 days in the period 20 September to 4 October 1979 (equinox, solar maximum). Both the receiver and the transmitter had their frequencies/phases controlled by cesium-beam frequency standards.

Figure 3 shows the results from LWPC nighttime calculations for the four Omega frequencies reported by Kikuchi at Inubo for appropriate values of *H'* (in the range 82-87 km) and β (in the range 0.50-0.80 km^{-1}). The phases are from LWPC's standard output in degrees (where the phase values increase when the ionospheric height lowers, e.g. during a solar flare, and decrease when the ionospheric height increases, e.g. in going from day to night). The text box, near the bottom of each of these panels, shows the phases calculated by LWPC for the appropriate panel frequency near *path mid-day* for the (equinoctial) dates shown. The results of these LWPC calculations are given for both solar minimum (using the daytime *H'* and β values determined by *McRae and Thomson*, [2000]) and solar maximum (using the daytime *H'* and β values determined by *Thomson*, [1993]). Also shown, in each text box, is the observed difference in phase between day and night from the observations of *Kikuchi* [1983, Table 2]. These observed differences are then combined with the LWPC-calculated solar maximum values (since 1979 was solar maximum) in the text boxes to effectively give the observed nighttime phase (in LWPC degrees) shown as thick bold horizontal straight lines.

It can thus be seen, that *H'* = 84-85km and $\beta \sim$ 0.65 km^{-1} give reasonable agreement between the observed phases and modeling for this 6.1 Mm, all-sea path. The agreement seems to be somewhat better for *H'* nearer 84 km for this solar maximum case (rather than the 85 km found at solar minimum), consistent with the rather tentative solar cycle change suggestion of *Thomson et al.* [2007]. The agreement is perhaps poorest at 11.333 kHz, for which frequency Kikuchi suggested the unusually small diurnal phase shift might be caused by “experimental errors”. This seems quite possible given there were only 3 days of observations at this frequency. No amplitude measurements were available for this path.

2.3 NWC, Exmouth, Australia, amplitudes at Antananarivo, Madagascar.

Lynn [1971] recorded the diurnal amplitude changes over the 6.9 Mm all-sea path NWC, Exmouth, Australia, to Antananarivo, Madagascar, on four frequencies (one at a time) during the period 1 February to 25 September 1968 (ie solar maximum, around the winter solstice). Figure 4 shows results from LWPC calculations for NWC on the four frequencies reported by *Lynn* [1971] for various values of *H'* (in the range 83-87 km) and β (in the range 0.50-0.90 km^{-1}). The amplitudes are from LWPC's standard output in dB above 1 μV/m for NWC’s reported radiated power of 1 MW.

Lynn reported only the average night-to-day amplitude *ratios* (in dB); no diurnal plots were given. Lynn reports that these ratios were determined, at each frequency, by taking hourly estimates of signal level for 5 days at times when the path was entirely illuminated or in complete darkness. Because the daytime amplitude is greatest at mid-day, Lynn’s (averaged) daytime amplitudes will have been lower than his mid-day values. This has been allowed for here by using LWPC with the (solar maximum) *H'* and β values, as functions of solar zenith angle, from *Thomson* [1993]; the resulting equivalent mid-day amplitudes are used in Figure 4. Two difficulties arose which will have reduced the accuracy a little: firstly, some of these daytime calculations needed to be done for solar zenith angles with the sun nearer dawn or dusk than fully calibrated, and, secondly, Lynn did not report the time of year (and hence average daytime solar zenith angle) at which each frequency was recorded. However, it is likely that Lynn’s observations are none-the-less sufficiently accurate for the present purpose to allow a useful comparison here. It can be seen, in Figure 4, that *H'* = 84-85 km and β = 0.6-0.8 km^{-1} (broadly in line with the values found by *Thomson et al.*, [2007]) give reasonable agreement between the observed amplitudes and modeling for this 6.9 Mm, relatively low-latitude (~30º geomagnetic), all-sea path. No phase measurements were available.

2.4 NLK, Seattle, phase at Hyogo, Japan

Muraoka [1979] recorded the diurnal phase changes over the 8.0 Mm all-sea path, across the North Pacific, from NLK (18.6 kHz), Seattle, to Nishinomiya, Hyogo, Japan, during the period June 1974 to November 1976.

Figure 5 shows the appropriate LWPC-calculated nighttime phases for a range of *H'* and β. The text box gives the phases calculated by LWPC near *path mid-day* for the (mid-summer) dates shown together with the observed day-night phase difference from the observations of *Muraoka* [1979, Figs. 3 & 4]. The nighttime phases, used to find the day-night difference, included those from all year except the 3-4 summer months because, for the highest latitude parts of the mid-summer, nighttime path, the sun would have been only ~10º below the horizon. The resulting comparison of mid-day, mid-summer phases with nighttime phases during the rest of the year was possible only because of the cesium-beam frequency controls for both transmitter and receiver, and *Muraoka* using these to appropriately correct for the 20-40 μs measured annual phase drifts. As for the other paths, the observed day-night differences were then combined with the LWPC-calculated mid-day, solar minimum phase (since 1974-76 was near solar minimum) to give the effective observed nighttime phase (in LWPC degrees) shown as a thick bold horizontal straight line. From the scatter in Muraoka's phases from night to night, a reasonable estimate of the likely error in this mean observed nighttime phase would be ~ ±15°.

It can thus be seen, that *H'* = 85.1 km and β = 0.63 km^{-1} (the values found by *Thomson et al.*, [2007]) give good agreement between the observed phases and modeling for this 8.0 Mm all-sea path. No nighttime amplitude measurements were available.

2.5 NBA, Panama Canal Zone, to Boulder, Colorado

Chilton et al. [1964] recorded amplitudes and phases for the 4.3 Mm part-land, part-sea path from NBA (18.0 kHz), Panama Canal Zone, to Boulder, Colorado, USA, during the period April 1962 to June 1963.

Figure 6 shows LWPC-calculated nighttime phases and amplitudes (in dB above 1 μV/m for an arbitrary 110 kW of radiated power) for an appropriate range of H' and β. The text boxes give the amplitudes (upper panel) and phases (lower panel) calculated by LWPC near *path mid-day* for the for the (near) summer dates shown together with the observed day-night amplitude and phase changes from the observations of *Chilton et al.* [1964]. The phase changes used were for the months of April-August 1962 and April-June 1963 from *Chilton's* Fig 7. Amplitudes were reported only for the month of April 1963 (*Chilton's* Fig. 3) so this month alone provided the day-night amplitude change. The hour to hour mean nighttime amplitude variations suggest that the error in the mean day-night amplitude change is probably less than ~ ±1 dB. For phase, the variations from month to month indicate the mean observed phase change error is ~ ±15°.

As before, the observed nighttime amplitudes and phases have been found by combining the experimentally determined day-night changes with the calculated daytime values (given in the text panels). As can be seen, H' = 85.1 km and β = 0.63 km^{-1} (the values found by *Thomson et al.*, [2007]) give reasonable agreement between the observations and modeling for both amplitude and phase for this 4.3 Mm path about one third of which is over land (the continental USA) and about two thirds over the sea.

3. Transequatorial Observations and Modeling

3.1 Background

It has long been recognized that there has appeared to be anomalous effects observed in the nighttime amplitudes and/or phases of VLF radio signals which cross the geomagnetic equator [e.g. *Chilton et al*., 1964; *Lynn* 1967, 1969, 1975; *Araki et al*., 1969; *Araki*, 1973; *Kikuchi*, 1983]. These effects were anomalous in terms of observations: the behavior observed near the equator was distinctly different from that observed elsewhere. However, these studies did not have appropriate VLF propagation code available, such as MODEFNDR or LWPC, to take into account the (changing) magnetic field parameters (particularly dip, and azimuth) needed to model such paths. In particular, Wait's nighttime VLF propagation calculations, resulting in the widely used tables of *Wait and Spies* [1964, supplement 2], included no dip or azimuth dependence. In contrast, the later VLF propagation code, developed by the US Navy at San Diego (based on earlier work by Budden), found that the calculated effects of both azimuth and dip, particularly near the geomagnetic equator at night, were quite marked [*Pappert and Bickel,* 1970; *Bickel et al.,* 1970]; for example, for the first order mode at 21.8 kHz, the nighttime attenuation to the east from Hawaii (~20° geomagnetic latitude) was calculated to be ~0.4 dB/Mm while to the west it was ~1.8 dB/Mm [*Pappert and Bickel,* 1970]. At this time both the (NOSC, San Diego) calculations and the observations agreed that VLF propagation near the equator was markedly different from elsewhere; however there were very few comparisons made to check that this new transequatorial modeling did, in fact, agree with the observed ‘anomalous’ transequatorial behavior. A contributing factor to this lack of comparisons was that many of the (‘anomalous’) equatorial observations related to the timing of dawn/dusk modal minima which are very hard to model accurately without detailed knowledge of the time dependence of the dawn/dusk D-region electron densities. Lack of availability of the NOSC (San Diego) code during the years of the anomalous transequatorial observations may well have also been a contributing factor to the lack of comparisons. In this section we now compare several such transequatorial VLF observations with LWPC modeling using a range of values of *H’* and β.

3.2 Omega Japan Amplitudes and Phases at Dunedin, NZ

Figure 7 shows the observed amplitudes and phases (relative to arbitrary base levels), as functions of hours UT, for the 13.6 kHz signals from Omega Japan after propagating 9.8 Mm across the equator and Pacific Ocean to Dunedin, New Zealand (a nearly all-sea path), for the period 19-27 September 1996. These recordings, and all other *phase* and amplitude recordings at Dunedin reported here, were made on AbsPAL receivers [*Thomson et al.*, 2005, 2007; *McRae and Thomson*, 2000, 2004, and references therein]. The average mid-day (~02 UT) and night (~14 UT) amplitude and phase values in Figure 7 are indicated by the horizontal straight lines.

In Figure 8, the upper two panels show results for LWPC calculations for Omega Japan on 13.6 kHz to Dunedin for the usual values of *H'* (in the range 83-87 km) and β (in the range 0.50-0.70 km^{-1}), appropriate for night time propagation. The amplitudes and phases are from LWPC's standard output with the amplitudes being in dB above 1 μV/m, assuming the normal Omega radiated power of 10 kW. As previously, the text box, near the bottom of each of these panels, shows daytime amplitudes and phases calculated by LWPC for *path mid-day* for the (equinoctial) date shown. Also shown, in each text box, is the observed difference in phase or amplitude between day and night, as read from the appropriate lines in Figure 7. As previously, these observed differences were then combined with the LWPC-calculated solar minimum values (since 1996 was solar minimum) in the text boxes to effectively give the observed nighttime amplitude and observed nighttime phase (in LWPC units) shown as thick bold horizontal straight lines, in each of the upper two panels of Figure 8. It can thus be seen, that there is good agreement in phase for the usual non-equatorial value H' ~ 85 km but that the measured amplitude is ~5 dB lower for this equator-crossing path than would have been expected from the usual non-equatorial value $\beta = 0.63$ km^{-1} (or indeed any similar value of β).

The lower two panels in Figure 8 show the results for the same transequatorial Omega Japan to Dunedin path as the upper two panels, except for 10.2 kHz rather than 13.6 kHz. Again, the measured amplitude is much lower, ~6.5 dB, for this transequatorial path than would have been expected from the use of the normal non-equatorial value of $\beta = 0.63$ km^{-1} (or indeed any even moderately similar value of β). Similar results (not shown here) were found for 12.8 kHz (the frequency ‘unique’ to Omega Japan) on this same transequatorial path: the measured nighttime amplitude was ~5.5 dB lower than would have been expected from the use of the normal non-equatorial value of β.

3.3 JJI (22.2 kHz), Kyushu, Japan, to Dunedin, NZ

Amplitude only, for JJI (22.2 kHz), Kyushu, Japan, after propagating 9.5 Mm across the equator and the Pacific ocean to Dunedin, N.Z., was recorded during the period 10 March to 4 April 1998 using a SCODAR receiver [*Thomson*, 1985]. These amplitudes, in dB, are shown in the top panel of Figure 9 and, in the bottom panel, these observed amplitudes are compared, in the same way as for the previous paths, with those calculated (in dB above 1 µV/m, for 175 kW radiated) from a range of D-region ionospheric parameters. Again, as for Omega Japan to Dunedin, the observed amplitude is much lower (~8 dB) for this transequatorial path than would have been expected from the normal non-equatorial value of β = 0.63 km^{-1} (or indeed any moderately similar value of β).

3.4 NWC, Australia, Amplitudes and Phases in Japan

In last two sub-sections, the propagation was southwards across the equator (and slightly to the East). We now consider propagation northwards across the equator (and also slightly to the East). *Araki et al.* [1969] recorded diurnal amplitudes and phases for the 6.7 Mm nearly all-sea path from NWC, North West Cape, Australia to Uji, Kyoto, Japan, during the periods 31 July to 7 August and 7-14 August 1968 on 15.5 kHz and 22.3 kHz respectively. In addition, *Araki* [1972], using observations of NWC at Inubo, Japan, in 1968 [*Ishii et al*. 1968], noted the nighttime amplitude at 19.8 kHz, on this 7.0 Mm path, was particularly low, being typically about 10 dB lower than the daytime amplitude.

Figure 10 shows LWPC-calculated nighttime amplitudes (in dB >1µV/m) and phases at Uji for 22.3 kHz and 15.5 kHz, for 1 MW radiated, using an appropriate range of *H'* and β. As before, the text boxes give the amplitudes (upper panels) and phases (lower panels) as calculated by LWPC near path mid-day together with the observed day-night amplitude and phase changes from *Araki et al*. [1969]. Again the "observed" nighttime amplitudes and phases have been found by combining the experimentally observed day-night changes with the calculated daytime values (given in the text panels). Similarly, Figure 11 shows the results for NWC on 19.8 kHz at Inubo, using the observations reported by *Araki* [1972].

In Figures 10 and 11 it can been seen that the observed amplitudes of NWC at night are again appreciably lower on this transequatorial path than would have been expected from the usual nighttime values of *H'* and β which give good predictions on non-equatorial paths. For 22.3 kHz these observed transequatorial nighttime amplitudes are a significant 4-5 dB lower for *H'* = 84-85 km, while at 15.5 kHz they are a marginal 2.5-3.5 dB lower, and at 19.8 kHz they are a marked ~9 dB lower than for the amplitudes expected from the normal non-equatorial β = 0.60-0.70 km^{-1}. The observed phases, at best, agree only marginally with the values calculated from the normal non-equatorial (solar maximum) *H'* = 84-85 km. Based on the variations of the monthly mean phases at Inubo, the likely observed nighttime phase error will be about ±30°. For the amplitudes, no variation information was given.

3.5 Propagation from Hawaii across the Equator, southward and slightly westward, to Dunedin, NZ

The top two panels on the left of Figure 12 show the amplitudes and phases of Omega Hawaii on 10.2 kHz (relative to arbitrary base levels) from our receivers at Dunedin, NZ, during the period 13-30 March 1996. This path crosses the magnetic equator in a direction slightly *westwards* of North-to-South (~191° magnetic azimuth). The propagation here is appreciably more variable than for Omega Japan to Dunedin (Figure 7) which crosses the magnetic equator in a direction somewhat *eastwards* of North-to-South (~155° magnetic azimuth). While some of this additional variability will be due to the slightly lower signal-to-noise ratio of Omega Hawaii at

Dunedin (partly due to the higher attenuation to the west and partly to the lower frequency), most of the variability seems to be due to crossing the equator in the unfavorable, (slightly) to-the-west direction.

The other six panels of Figure 12 show LWPC-calculated nighttime amplitudes and phases for Omega Hawaii (radiating 10 kW) received at Dunedin on 10.2 kHz, 11.8 kHz (the ‘unique’ frequency) and 13.6 kHz using appropriate ranges of H' and β. As before, the text boxes give the amplitudes (upper panels) and phases (lower panels) as calculated by LWPC near path mid-day together with the observed day-night amplitude and phase changes from the observations at Dunedin (such as those shown, for 10.2 kHz, in the two top left panels). As usual, the “observed” nighttime amplitudes and phases have been found by combining the observed day-night changes with the calculated daytime values (from the text panels). Similarly, Figure 13 shows the results for NPM, Hawaii, on 21.4 kHz (2007) and 23.4 kHz (1996) at Dunedin. (The calculated amplitudes are in dB >1 μV/m for 400 kW radiated at 21.4 kHz. For 23.4 kHz the normal nominal 600 kW was used, although NPM was temporarily on half-power during the period shown; this has no effect on the amplitude differences.) As can be seen in the top left panel of Figure 12, the standard deviation in the nighttime phase of Omega Hawaii on 10.2 kHz is about 5 dB and so the error in the mean for the ~2 weeks data will be ~ ±1.2 dB. For NPM, where there is one week’s data, the corresponding errors are ~ ±1.5 dB at 23.4 kHz and ~ ±2 dB at 21.4 kHz. For the phases, the corresponding errors in the means are ~ ±15°

As can be seen in Figures 12 and 13, the observed amplitudes from Hawaii at night, on this transequatorial path, agree (approximately) for just 2 of the 5 frequencies shown, 10.2kHz and 21.4 kHz, with what would be expected from the usual (non-equatorial) nighttime values of *H'* and β. Also available and compared, but not shown here, were results for 11.05 kHz and 11 1/3 kHz for Omega Hawaii to Dunedin, thus making 7 frequencies, in total, available for this path. At 13.6 kHz the observed amplitude at night was *lower* than that calculated by ~4 dB, while for the other 4 frequencies the observed amplitudes were *higher* than calculated: by ~4 dB at 11.05 kHz, by ~7 dB at 11 1/3 kHz, by ~4 dB at 11.8 kHz and by ~10-12 dB at 23.4 kHz. For all these latter 4 frequencies, the calculations showed some form of amplitude minimum near *H'* ~ 85 km and β ~ 0.65 km $^{-1}$ (as in the appropriate panels of Figures 12 and 13), which quite likely accentuated the inconsistency with the observations.

The calculated nighttime phases agree or nearly agree with observations for three of the 7 frequencies: 13.6 kHz, 21.4 kHz and 23.4 kHz. For the other four frequencies, the day-night phase shift observed was less than that modeled: by ~90° at 10.2 kHz, by ~100° at 11.05 kHz, by ~75° at 11.333 kHz and by ~30° at 11.8 kHz - the last of these being possibly only a marginally significant difference.

3.6 NBA, Panama, across the equator to Tucuman, Argentina

Chilton et al. [1964] recorded amplitudes and phases for the 4.3 Mm nearly all-land path from NBA (18.0 kHz), Panama Canal Zone, to Tucuman, Argentina, during the months April, May and June 1963. LWPC calculations using *H'* = 84-85 km and β = 0.60-0.70 km^{-1} gave a diurnal phase shift of ~110° in near agreement with the average observed phase shift of ~128° but the observed amplitude was ~13 dB below that given by the LWPC calculation. Clearly, at least at first sight, this appears to be another transequatorial case where the modeled and observed amplitude are very different. However, it must be noted that this path is also over nearly all-land, parts of which are of medium to low conductivity, and, in particular, significant parts are over very high mountains (in the Andes). Thus, in practice, the terrain may well be playing a significant part in the scattering or attenuation of the waves for this case; in contrast, the LWPC modeling assumes the surface of the Earth is a smooth sphere of constant radius, taking no account of re-radiation or scattering by mountains. LWPC contains one surface conductivity estimate for each square degree of latitude/longitude (~100 km square) and, while this can potentially give reasonable estimates for the attenuation for smoothly changing (flat) ground over long paths, much greater uncertainty exists in rapidly changing mountain regions. Steep slopes and sharp conductivity boundaries can be expected to cause scattering away from the rather narrow, favored transmission elevation angles and so, in modal terminology, cause mode-conversion into typically higher attenuated modes.

4. Discussion, Summary and Conclusions

Thomson et al. [2007] showed that their VLF radio observations, particularly over six nearly all-sea paths, were consistent with the lower edge of the ionosphere's nighttime D-region having electron densities and collision frequencies defined by the parameters, H' = 85.1 km and β = 0.63 km^{-1}, for mid-latitudes, *away from the equator*. Here, in section 2, we have shown that these same parameters are consistent with the VLF radio observations of others, reported in the literature over the last forty years or so, for nighttime mid-latitudes, away from the equator.

However, in section 3, we have also found that these mid-latitude nighttime ionospheric parameters typically do *not* give good agreement for *transequatorial* paths. While significant disagreements occur for both phase and amplitude on these paths, the amplitude disagreements are typically more marked. Generally the observed amplitudes are lower than the non-equatorial D-region parameters would predict. However, when these parameters predict a (near) modal minimum at the receiver, then the observed transequatorial amplitude is typically larger than the modeled value.

As could be seen in the figures in section 3, in many transequatorial cases the values of *H'* and β (if any) that would be needed to get a fit with modeling would be quite unrealistic. This could possibly be due to some unexpected problem with the LWPC propagation code at or near the nighttime equator. The likelihood of this is somewhat reduced, though certainly not eliminated, by comparison with LWPC's predecessor code, MODEFNDR. Although LWPC appears to have been written to some extent afresh, it still uses largely the same algorithms as MODEFNDR and the two generally agree very well in conditions where comparisons are readily possible. The most important difference, though, is that, while MODEFNDR uses one set of parameters (magnetic azimuth, magnetic dip etc) to find one set of modes for the whole of the propagation path length, LWPC divides the path into (distance) segments, each with its own (magnetic) parameters and then finds a set of modes for each of these segments. The LWPC code then performs mode conversions as it moves from one segment to the next along the propagation path.

Segmentation and mode conversion are more important on some paths than others; it generally depends on how fast the parameters and resulting reflection coefficients (and hence the allowed modes) are changing. The original LWPC was programmed to choose its own segment size according to how rapidly it perceived the propagation parameters to be changing along the path. We have altered our code so that we can set a maximum segment size (usually relatively small but can be set as large as the full path length). We have generally run LWPC for this study with a maximum segment length of 100 km, which is considerably smaller than in original LWPC. We have done this because it greatly reduces the risk of significantly increased error due to having segments too long; the increased computation time is much less of an issue now than a couple of decades or so ago when LWPC was designed. However, there are a few paths where even 100 km is too long; for the Hawaii to Dunedin nighttime paths here we generally used 20 km. It might possibly be thought that such short segment lengths would require so many mode conversions (~8000km/20km = 400 for the Hawaii-Dunedin path) that accuracy could be compromised. However, a simple test showed there was little difference in the final amplitudes and phases calculated, even in the most sensitive cases, for segment sizes in the range ~5-25 km.

As mentioned, some paths are not very greatly affected by segmentation and mode conversion. Japan to New Zealand, with its somewhat eastward equator crossing, is such a case. We tested this by turning off mode conversion in LWPC and finding no great changes. MODEFNDR, with just one set of appropriate (average) magnetic parameters, was also found to give very similar transequatorial nighttime attenuations to full LWPC. A Wave Hop code was also available based on *Berry and Herman* [1971]. For Japan to Dunedin, this too gave nighttime amplitudes closer to those of LWPC and MODEFNDR (within ~1 dB, using the same values of *H’* and β) rather than the observed amplitudes which were ~5 to 8 dB lower than those from LWPC as shown in Figures 7-9. Wave hop codes mainly use very different algorithms from modal codes such as LWPC and MODEFNDR. *Jones and Mowforth* [1981] have shown reasonable agreement between their wave hop and waveguide modal codes for a number of mid-latitude conditions. We have also found typically good agreement (<~2 dB in amplitude) between our Wave Hop code and LWPC, although there are some discrepancies not fully understood. Like MODEFNDR, our Wave Hop code has no variation of (magnetic) parameters along the path and no equivalent of mode conversion. None-the-less, the relatively near agreement of LWPC with Wave Hop indicates fairly strongly that the discrepancy between calculations and observations for transequatorial paths is probably not a code (algorithm) problem; it is more likely to be a real geophysical effect.

It thus seems much more likely this transequatorial effect is due to some feature of the bottom edge of the (D-region of the) equatorial nighttime ionosphere. *Fejer et al.* [1975] observed significant 50 MHz radar backscatter from type 2 irregularities (thought to be associated with the gradient drift instability) down to 93 km at Jicamarca both by day and by night. Similar equatorial backscatter was reported by *Tsunoda and Ecklund* [1999] down to about 89 km. Such irregularities in the nighttime equatorial ionosphere may well be penetrating sufficiently below ~90 km altitude resulting in the scattering of the VLF radio energy as it passes the equator. In general, VLF waves which reach distant receivers in the Earth-ionosphere waveguide are those which have traveled with optimum (near grazing) incidence angles (elevation angles) because these have the lowest attenuations. (In modal terms they have traveled in low-order modes.) Scattering at a rough surface, such as from a perturbed equatorial D-region, will scatter wave energy into angles of incidence which will require (many) more hops, and hence significantly more attenuation, to reach the receiver. (In modal terms, the roughness will cause mode-conversion at the equator into higher order modes with higher attenuation rates. The strong and rapid VLF amplitude fluctuations with distance reported by *Bickel et al.*, [1970] just south of the equator on a flight along the transequatorial NPM, Hawaii, to Samoa path are strongly indicative of interference with such higher order modes.) Hence any 'roughness' of the lower edge of the equatorial D-region will generally cause extra attenuation and so lower amplitudes at the receiver. However, in cases where LWPC would have predicted a (low amplitude) modal minimum at the receiver (in the absence of equatorial roughness) the equatorial mode conversion could well alter the modal mix arriving at the receiver so as to fill out any minimum that the code was otherwise predicting. In these much less common cases the amplitude at the receiver would be observed to be higher than LWPC's (low, modal minimum) predictions because of the transequatorial effects.

Acknowledgement. We thank english.freemap.jp for the use of their free world map.

References

Araki, T., S. Kitayama and S. Kato (1969), Transequatorial reception of VLF radio waves from Australia, *Radio Sci. 4*(4)**,** 367-369.

Araki, T. (1973), Anomalous diurnal changes of transequatorial VLF radio waves, *J. Atmos. Terr. Phys., 35*, 693-703.

Berry, L.A. and J.E. Herman (1971), A wave hop program for an anisotropic ionosphere, OT/ITS Research Report 11, Boulder, Co.

Bickel, J. E., J. A. Ferguson, and G. V. Stanley (1970), Experimental observation of magnetic field effects on VLF propagation at night, *Radio Sci. 5***,** 19-25.

CCIR (1990). *Radio propagation and circuit performance at frequencies below about 30 kHz.* Document 6/1030-E (30 October 1989), Report 895-1 (Mod F, 29 pages), Comite Consultatif International des Radioommunications, XVII Plenary Assembly, Dusseldorf.

Cheng, Z., S. A. Cummer, D. N. Baker, S. G. Kanekal (2006), Nighttime *D* region electron density profiles and variabilities inferred from broadband measurements using VLF radio emissions from lightning, *J. Geophys. Res., 111*, A05302, doi:10.1029/2005JA011308.

Chilton, C.J., A.H. Diede, S.M. Radicella (1964), Transequatorial reception of a very-low frequency transmission, *J. Geophys. Res.*,*69*(7), 1319-1327.

Cummer, S. A., U. S. Inan, and T. F. Bell (1998), Ionospheric *D* region remote sensing using VLF radio atmospherics, *Radio Sci., 33*(6), 1781-1792.

Fejer, B.G., D.T. Farley, B.B. Balsley and R.F. Woodman (1975), Vertical structure of the VHF backscattering region in the equatorial electrojet and the gradient drift instability, *J. Geophys. Res.*,*80*(10), 1313-1324.

Ferguson, J. A. (1980), Ionospheric profiles for predicting nighttime VLF/LF propagation, *Naval Ocean Systems Center Tech. Rep. NOSC/TR 530, NTIS Accession.ADA085399*. Natl. Tech. Inf. Serv. Springfield, VA 22161, USA.

Ferguson, J. A. (1995), Ionospheric model validation at VLF and LF, *Radio Sci.*, *30*(3), 775-782.

Ferguson, J. A. and F. P. Snyder (1990), Computer programs for assessment of long wavelength radio communications, version 1.0: full FORTRAN code user's guide, *Naval Ocean Systems Center Tech. Doc. 1773, DTIC AD-B144 839*, Defense Tech. Inf. Cent., Alexandria, Va.

Jones, T.B. and K. Mowforth (1981), A review of the analytical techniques for determining the phase and amplitude of a VLF radio wave propagating in the Earth-ionosphere waveguide, *AGARD Conf. Proc., 305*(16), 1-16 (ISBN 92-835-0311-2).

Kikuchi, T. (1983), Anomalous diurnal phase shifts of Omega VLF waves (10-14 kHz) on the east-west low latitude and transequatorial paths, *J. Atmos. Terr. Phys.*, *45*(11), 743-751.

Lynn, K.J.W. (1967), Anomalous sunrise effects observed on a long transequatorial VLF propagation path, *Radio Sci. 2*(6)**,** 521-530.

Lynn, K.J.W. (1969), Multisite observations of the VLF transequatorial propagation anomaly, *Radio Sci. 4*(3)**,** 203-211.

Lynn, K.J.W. (1971), Frequency dependence of VLF modal interference effects observed on east-west propagation paths, *J. Atmos. Terr. Phys., 33*, 951-958.

Lynn, K.J.W. (1975), The transequatorial reception of Omega (13.6 kHz) transmissions, *J. Atmos. Terr. Phys., 37*(10), 1395-1399.

McRae, W. M. and N. R. Thomson (2000), VLF phase and amplitude: daytime ionospheric parameters, *J. Atmos. Sol.-Terr. Phys.*, 62(7), 609-618.

McRae, W. M. and N. R. Thomson (2004), Solar flare induced ionospheric D-region enhancements from VLF phase and amplitude observations. *J. Atmos. Sol.-Terr. Phys.*, 66(1) 77-87.

Morfitt, D.G. (1977), Effective electron density distributions describing VLF/ELF propagation data,.*Naval Ocean Systems Center Tech. Rep., NOSC/TR 141, NTIS Accession ADA047508*, Natl. Tech. Inf. Serv. Springfield, VA.

Morfitt, D. G. and C. H. Shellman (1976), MODESRCH, an improved computer program for obtaining ELF/VLF/LF mode constants in an Earth-Ionosphere Waveguide. *Naval Electr. Lab. Cent. Interim Rep. 77T, NTIS Accession ADA032573*, Natl. Tech. Inf. Serv., Springfield, VA.

Morfitt, D.G., J.A. Ferguson, and F.P. Snyder (1981), Numerical modeling of the propagation medium at ELF/VLF/LF, *AGARD Conf. Proc., 305*(32*)*, 1-14 (ISBN 9-283-50311-2).

Muraoka, Y. (1979), Lower ionospheric disturbances observed in long-distance VLF transmission at middle latitude, *J. Atmos. Terr. Phys., 41*, 1031-1042.

Pappert, R. A. and J. E. Bickel (1970), Vertical and horizontal VLF fields excited by dipoles of arbitrary orientation and elevation, *Radio Sci. 5*, 1445-1452.

Pappert, R. A. and L. R. Hitney (1988), Empirical modeling of nighttime easterly and westerly VLF propagation in the Earth-ionosphere waveguide, *Radio Sci. 23*, 599-611.

Rhoads, F.J. and W.E. Garner (1967), An investigation of the modal interference of VLF radio waves, *Radio Sci.,2*(6), 539-546.

Thomson, N. R. (1985), Reflection of VLF radio waves from distant mountain ranges, *J. Atmos. Terr. Phys., 47*(4), 353-362.

Thomson, N. R. (1993), Experimental daytime VLF ionospheric parameters, *J. Atmos. Terr. Phys., 55*(2), 173-184.

Thomson, N. R. and M. A. Clilverd (2001), Solar flare induced ionospheric D-region enhancements from VLF amplitude observations. *J. Atmos. Sol-Terr. Phys.*, *63*(16), 1729-1737.

Thomson, N. R., C. J. Rodger and M. A. Clilverd (2005), Large solar flares and their ionosperic *D* region enhancements. *J. Geophys. Res.*, *110*(A6): A06306, doi:10.1029/2005JA011008.

Thomson, N. R, M. A. Clilverd and W. M. McRae (2007), Nighttime ionospheric D-region parameters from VLF phase and amplitude. *J. Geophys. Res.*, *112*(A7): A07304, doi:10.1029/2007JA012271.

Tsunoda, R.T. and W.L. Ecklund (1999), On the nature of radar echoes below 95 km during counter streaming in the equatorial electrojet, *Geophys. Res. Lett.*, 26(17), 2717-2720.

Wait, J.R. and K.P. Spies (1964), Characteristics of the Earth-ionosphere waveguide for VLF radio waves, *NBS Tech. Note 300*, National Bureau of Standards, Boulder, Co.

Figure Captions

Figure 1. The VLF transmitters (red squares), receivers (blue circles) and paths used here (see Table 1 for details). The geographic latitudes 0° and ±45° are indicated, as is the geomagnetic equator (green).

Figure 2. NPM, Hawaii, received at Washington DC. Comparisons of modeled and observed nighttime amplitudes at four frequencies.

Figure 3. Omega, Hawaii, received at Inubo, Japan. Comparisons of modeled and observed nighttime phases at four frequencies.

Figure 4. NWC, North West Cape, Australia, received at Antananarivo, Madagascar. Comparisons of modeled and observed nighttime amplitudes at four frequencies.

Figure 5. NLK, Seattle, received at Hyogo, Japan. Comparisons of nighttime modeled and observed phases.

Figure 6. NBA, Panama Canal Zone, received at Boulder, Colorado. Comparisons of nighttime modeled and observed amplitudes and phases.

Figure 7. Amplitude and phase of 13.6kHz from Omega Japan as measured at Dunedin, NZ, September 1996.

Figure 8. Omega Japan, measured at Dunedin, New Zealand. Comparisons of modeled and observed nighttime amplitudes and phases. Top panels: 13.6 kHz. Lower panels: 10.2 kHz.

Figure 9. JJI, Kyushu, Japan recorded at Dunedin, NZ.
Upper panel: Observed amplitudes (path at equinox).
Lower panel: Comparison with modeled amplitudes.

Figure 10. NWC, North West Cape, Australia, measured at Uji, Japan, after crossing the equator. Comparisons of nighttime modeled and observed amplitudes and phases. Top panels: 22.3 kHz. Lower panels: 15.5 kHz.

Figure 11. NWC, North West Cape, Australia, at Inubo, Japan, after crossing the equator. Comparisons of nighttime modeled and observed amplitudes and phases at 19.8 kHz.

Figure 12. Omega Hawaii measured at Dunedin, N.Z., after crossing the equator. The top two panels on the left show the diurnal variations of the amplitudes and phases at 10.2 kHz. The other six panels show comparisons of modeled and observed nighttime amplitudes and phases for 10.2 kHz, 11.8 kHz and 13.6 kHz.

Figure 13. NPM, Hawaii, measured at Dunedin, N.Z., after crossing the equator. Comparisons of modeled and observed nighttime amplitudes and phases. Top panels: 21.4 kHz. Lower panels: 23.4 kHz.

Transmitters	Latitude	Longitude	Mag.Lat.
JJI	32.2° N	130.8° E	25.4° N
NBA	9.1° N	79.7° W	21.0° N
NLK	48.2° N	121.9° W	53.8° N
NPM	21.4° N	158.2° W	21.4° N
NWC	21.8° S	114.2° E	32.8° S
Omega Hawaii	21.5° N	157.8° W	21.5° N
Omega Japan	34.6° N	129.5° E	28.0° N
Receivers			
Antananarivo	18.9° S	47.5° E	28.7° S
Boulder, CO	40.0° N	105.3° W	48.9° N
Dunedin, NZ	45.9° S	170.5° E	53.1° S
Hyogo, Japan	34.7° N	135.6° E	27.8° N
Inubo, Japan	35.7° N	140.9° E	28.7° N
Tucuman	26.8° S	65.3° W	14.3° S
Uji, Japan	34.9° N	135.8° E	28.0° N
Washington DC	39.0° N	77.0° W	49.9° N

Table 1. The transmitter and receiver locations in geographic latitude and longitude, and in geomagnetic latitude.

Freq kHz	Observed	Modeled
26.1	20.5	20.4
24.0	23.5	24.0
22.3	26.0	25.6
19.8	28.0	28.4

Table 2. Comparison of mid-day amplitude observations with modeling from LWPC for NPM, Hawaii, received near Washington DC. Amplitude units are dB > 1μV/m for 1 kW radiated power.

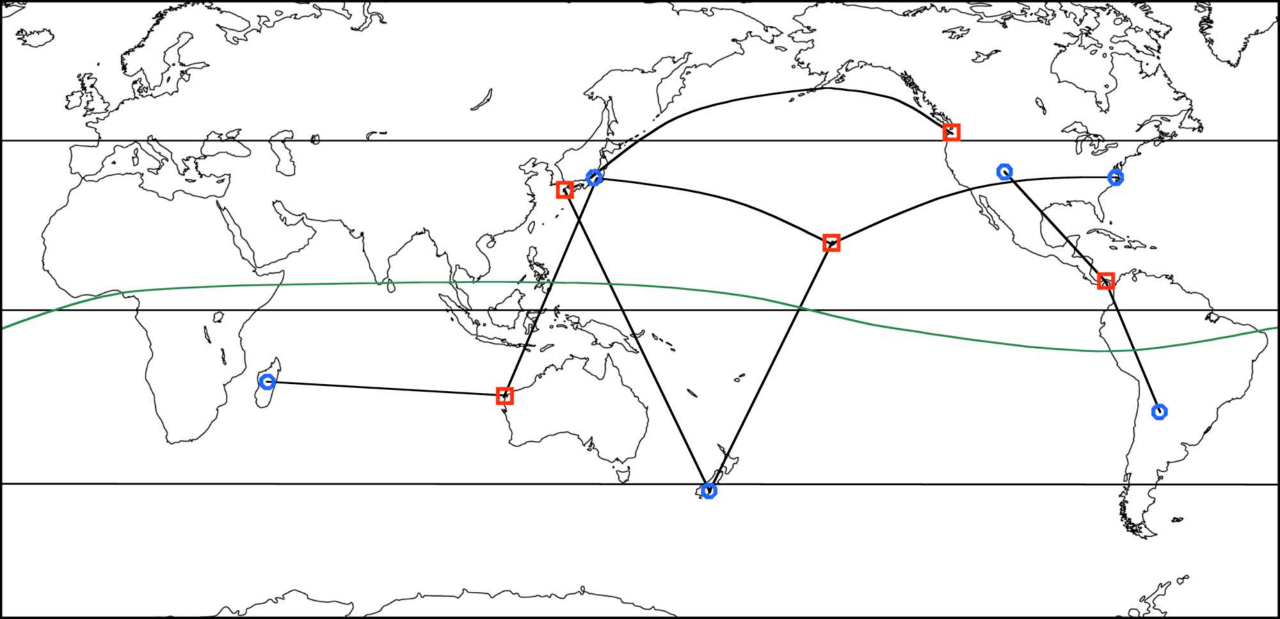

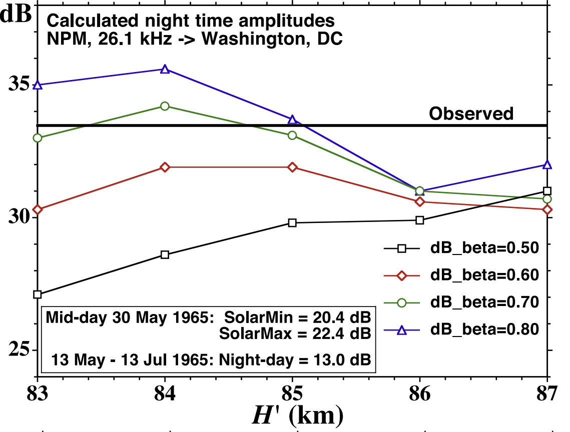
dB
Calculated night time amplitudes
NPM, 26.1 kHz -> Washington, DC
Observed
dB_beta=0.50
dB_beta=0.60
dB_beta=0.70
dB_beta=0.80
Mid-day 30 May 1965: SolarMin = 20.4 dB
SolarMax = 22.4 dB
13 May - 13 Jul 1965: Night-day = 13.0 dB
35
30
25
83
84
85
86
87
H' (km)

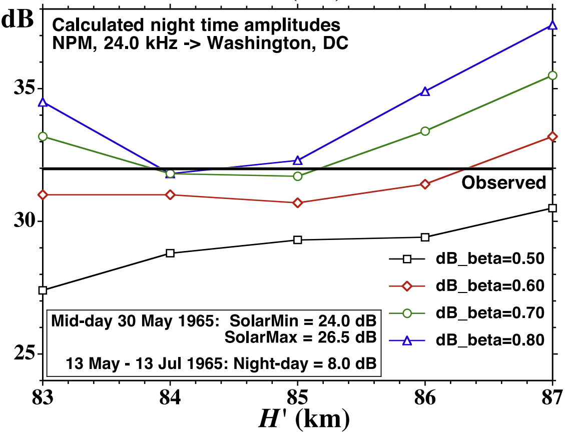
dB
Calculated night time amplitudes
NPM, 24.0 kHz -> Washington, DC
Observed
dB_beta=0.50
dB_beta=0.60
dB_beta=0.70
dB_beta=0.80
Mid-day 30 May 1965: SolarMin = 24.0 dB
SolarMax = 26.5 dB
13 May - 13 Jul 1965: Night-day = 8.0 dB
35
30
25
83
84
85
86
87
H' (km)

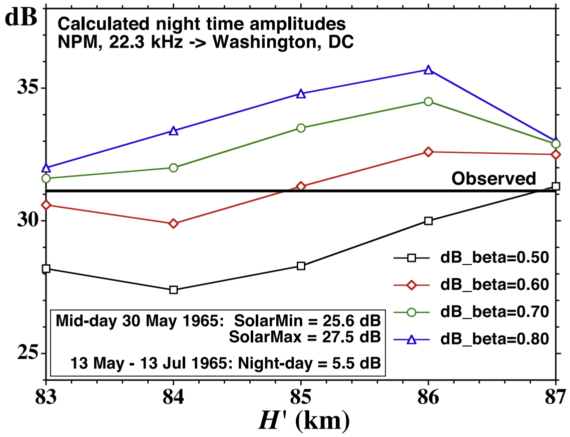
dB
Calculated night time amplitudes
NPM, 22.3 kHz -> Washington, DC
Observed
dB_beta=0.50
dB_beta=0.60
dB_beta=0.70
dB_beta=0.80
Mid-day 30 May 1965: SolarMin = 25.6 dB
SolarMax = 27.5 dB
13 May - 13 Jul 1965: Night-day = 5.5 dB
35
30
25
83
84
85
86
87
H' (km)

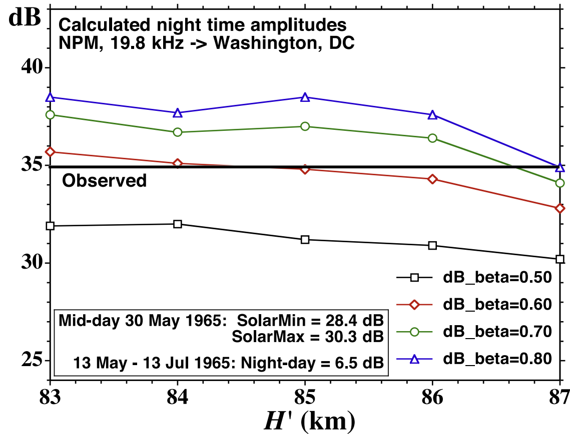
dB
Calculated night time amplitudes
NPM, 19.8 kHz -> Washington, DC
Observed
dB_beta=0.50
dB_beta=0.60
dB_beta=0.70
dB_beta=0.80
Mid-day 30 May 1965: SolarMin = 28.4 dB
SolarMax = 30.3 dB
13 May - 13 Jul 1965: Night-day = 6.5 dB
40
35
30
25
83
84
85
86
87
H' (km)

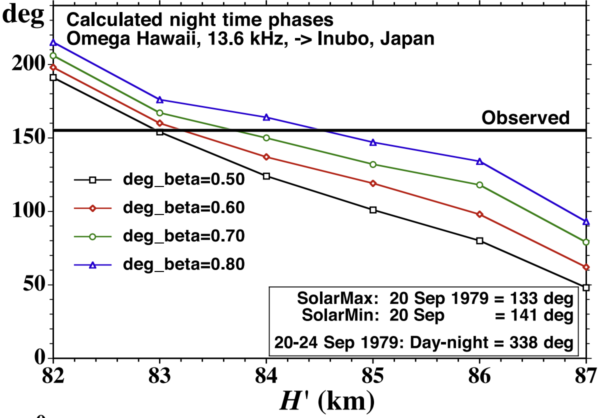
deg
Calculated night time phases
Omega Hawaii, 13.6 kHz, -> Inubo, Japan
Observed
deg_beta=0.50
deg_beta=0.60
deg_beta=0.70
deg_beta=0.80
SolarMax: 20 Sep 1979 = 133 deg
SolarMin: 20 Sep = 141 deg
20-24 Sep 1979: Day-night = 338 deg
0
50
100
150
200
82
83
84
85
86
87
H' (km)

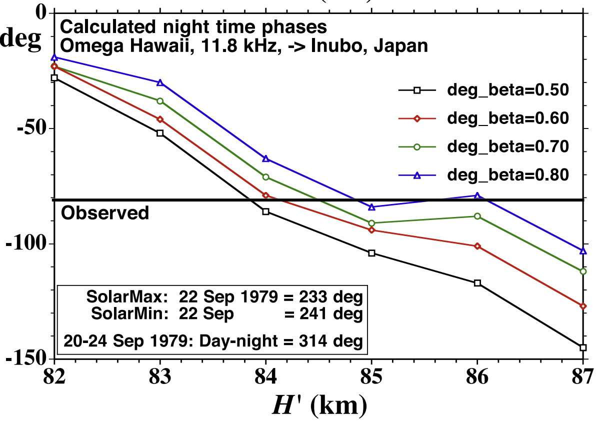
deg
Calculated night time phases
Omega Hawaii, 11.8 kHz, -> Inubo, Japan
deg_beta=0.50
deg_beta=0.60
deg_beta=0.70
deg_beta=0.80
Observed
SolarMax: 22 Sep 1979 = 233 deg
SolarMin: 22 Sep = 241 deg
20-24 Sep 1979: Day-night = 314 deg
0
-50
-100
-150
82
83
84
85
86
87
H' (km)

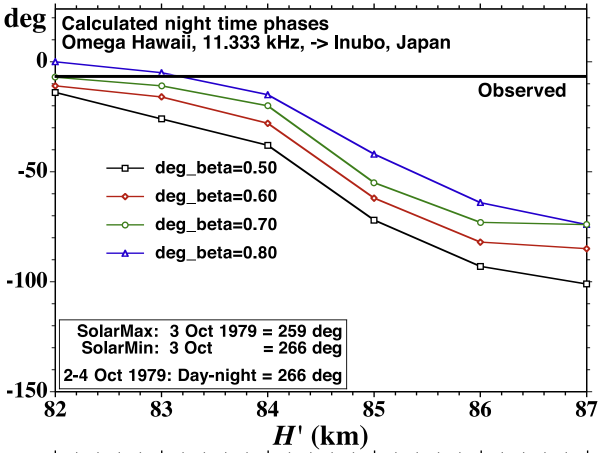
deg
Calculated night time phases
Omega Hawaii, 11.333 kHz, -> Inubo, Japan
Observed
deg_beta=0.50
deg_beta=0.60
deg_beta=0.70
deg_beta=0.80
SolarMax: 3 Oct 1979 = 259 deg
SolarMin: 3 Oct = 266 deg
2-4 Oct 1979: Day-night = 266 deg
0
-50
-100
-150
82
83
84
85
86
87
H' (km)

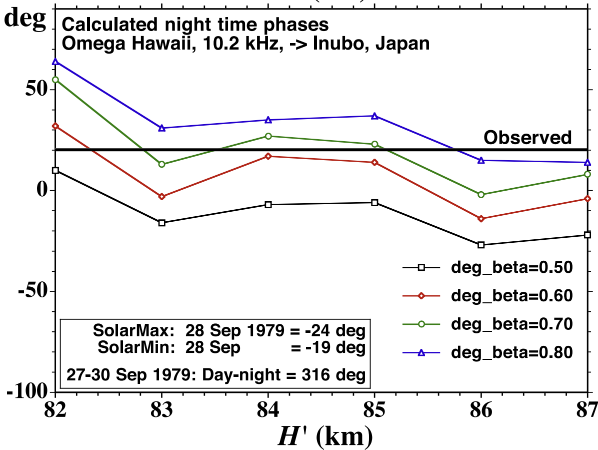
deg
Calculated night time phases
Omega Hawaii, 10.2 kHz, -> Inubo, Japan
Observed
deg_beta=0.50
deg_beta=0.60
deg_beta=0.70
deg_beta=0.80
SolarMax: 28 Sep 1979 = -24 deg
SolarMin: 28 Sep = -19 deg
27-30 Sep 1979: Day-night = 316 deg
50
0
-50
-100
82
83
84
85
86
87
H' (km)

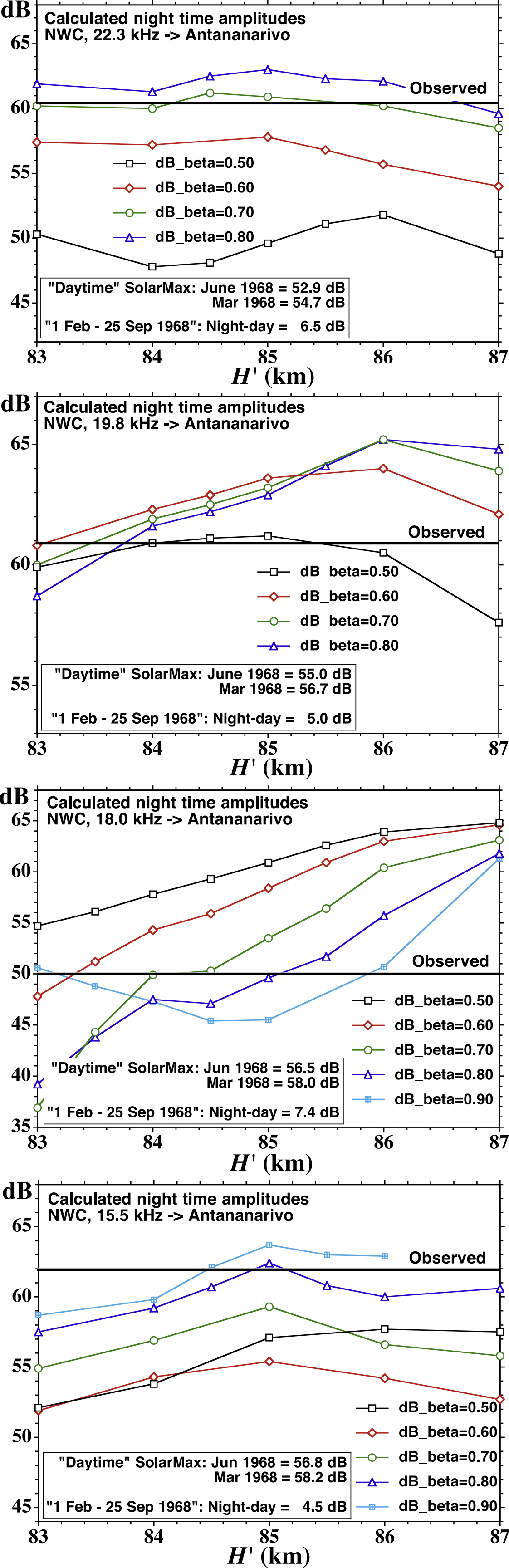

Calculated night time amplitudes
NWC, 22.3 kHz -> Antananarivo
Observed
dB_beta=0.50
dB_beta=0.60
dB_beta=0.70
dB_beta=0.80
"Daytime" SolarMax: June 1968 = 52.9 dB
Mar 1968 = 54.7 dB
"1 Feb - 25 Sep 1968": Night-day = 6.5 dB
dB
H' (km)
Calculated night time amplitudes
NWC, 19.8 kHz -> Antananarivo
Observed
dB_beta=0.50
dB_beta=0.60
dB_beta=0.70
dB_beta=0.80
"Daytime" SolarMax: June 1968 = 55.0 dB
Mar 1968 = 56.7 dB
"1 Feb - 25 Sep 1968": Night-day = 5.0 dB
dB
H' (km)
Calculated night time amplitudes
NWC, 18.0 kHz -> Antananarivo
Observed
dB_beta=0.50
dB_beta=0.60
dB_beta=0.70
dB_beta=0.80
dB_beta=0.90
"Daytime" SolarMax: Jun 1968 = 56.5 dB
Mar 1968 = 58.0 dB
"1 Feb - 25 Sep 1968": Night-day = 7.4 dB
dB
H' (km)
Calculated night time amplitudes
NWC, 15.5 kHz -> Antananarivo
Observed
dB_beta=0.50
dB_beta=0.60
dB_beta=0.70
dB_beta=0.80
dB_beta=0.90
"Daytime" SolarMax: Jun 1968 = 56.8 dB
Mar 1968 = 58.2 dB
"1 Feb - 25 Sep 1968": Night-day = 4.5 dB
dB
H' (km)

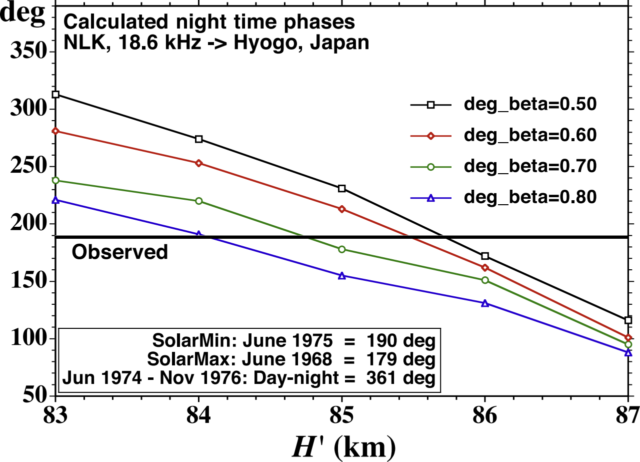

deg
Calculated night time phases
NLK, 18.6 kHz -> Hyogo, Japan
350
300
250
200
150
100
50
deg_beta=0.50
deg_beta=0.60
deg_beta=0.70
deg_beta=0.80
Observed
SolarMin: June 1975 = 190 deg
SolarMax: June 1968 = 179 deg
Jun 1974 - Nov 1976: Day-night = 361 deg
83
84
85
86
87
H' (km)

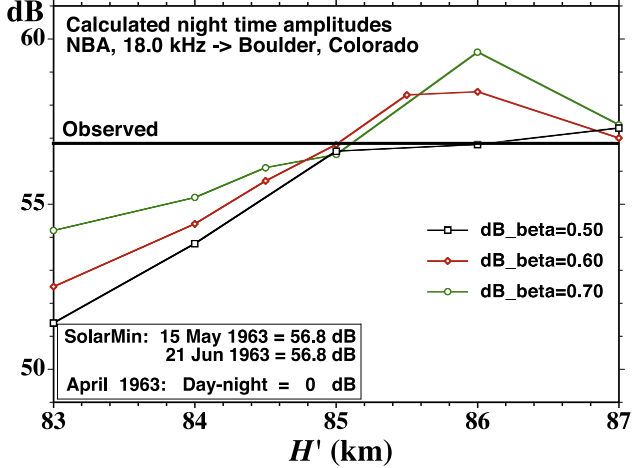
dB
Calculated night time amplitudes
NBA, 18.0 kHz -> Boulder, Colorado
Observed
dB_beta=0.50
dB_beta=0.60
dB_beta=0.70
SolarMin: 15 May 1963 = 56.8 dB
21 Jun 1963 = 56.8 dB
April 1963: Day-night = 0 dB
60
55
50
83
84
85
86
87
H' (km)

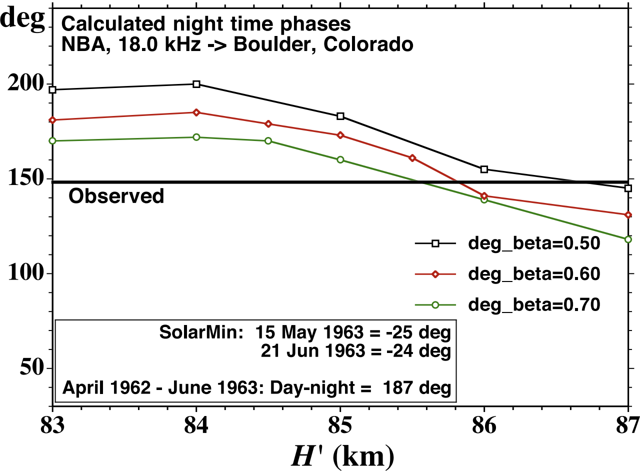
deg
Calculated night time phases
NBA, 18.0 kHz -> Boulder, Colorado
Observed
deg_beta=0.50
deg_beta=0.60
deg_beta=0.70
SolarMin: 15 May 1963 = -25 deg
21 Jun 1963 = -24 deg
April 1962 - June 1963: Day-night = 187 deg
200
150
100
50
83
84
85
86
87
H' (km)

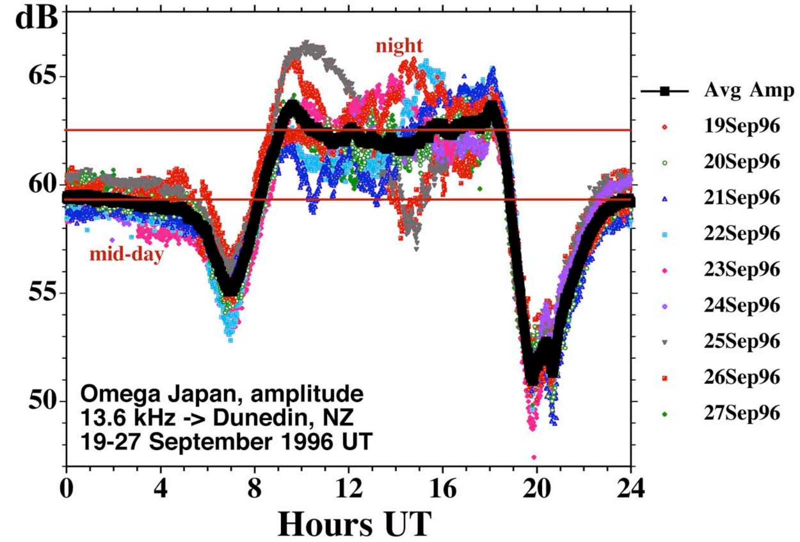
dB
65
60
55
50
night
mid-day
Avg Amp
19Sep96
20Sep96
21Sep96
22Sep96
23Sep96
24Sep96
25Sep96
26Sep96
27Sep96
Omega Japan, amplitude
13.6 kHz -> Dunedin, NZ
19-27 September 1996 UT
0
4
8
12
16
20
24
Hours UT

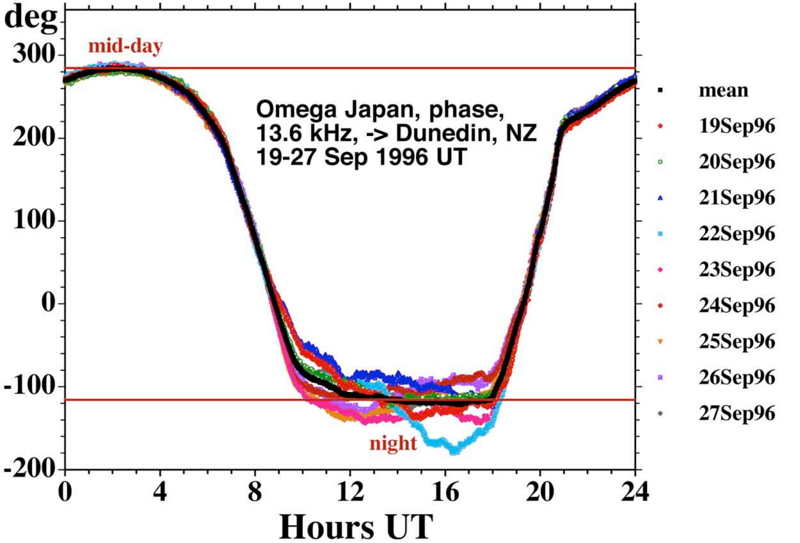
deg
300
200
100
0
-100
-200
mid-day
night
mean
19Sep96
20Sep96
21Sep96
22Sep96
23Sep96
24Sep96
25Sep96
26Sep96
27Sep96
Omega Japan, phase,
13.6 kHz, -> Dunedin, NZ
19-27 Sep 1996 UT
0
4
8
12
16
20
24
Hours UT

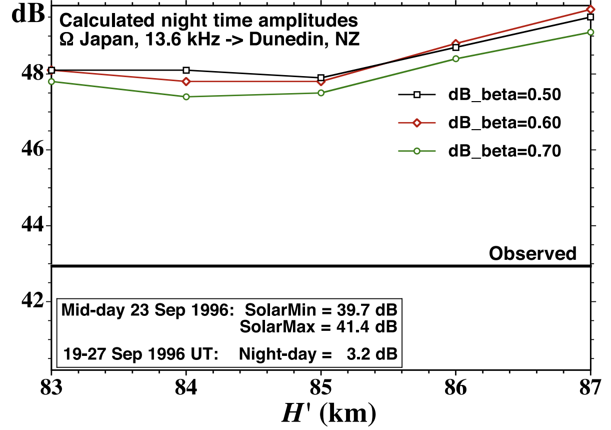
dB
Calculated night time amplitudes
Ω Japan, 13.6 kHz -> Dunedin, NZ
dB_beta=0.50
dB_beta=0.60
dB_beta=0.70
Observed
Mid-day 23 Sep 1996: SolarMin = 39.7 dB
SolarMax = 41.4 dB
19-27 Sep 1996 UT: Night-day = 3.2 dB
H' (km)

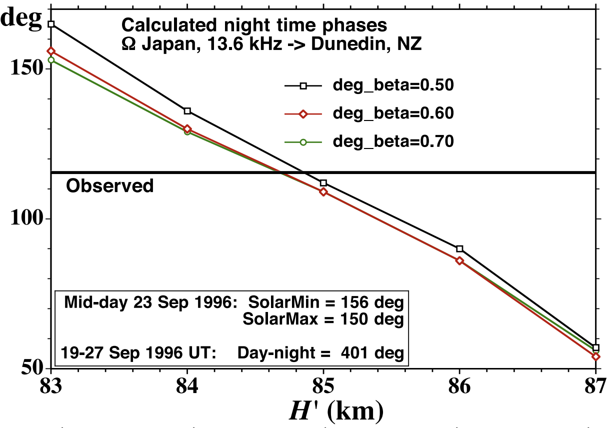
deg
Calculated night time phases
Ω Japan, 13.6 kHz -> Dunedin, NZ
deg_beta=0.50
deg_beta=0.60
deg_beta=0.70
Observed
Mid-day 23 Sep 1996: SolarMin = 156 deg
SolarMax = 150 deg
19-27 Sep 1996 UT: Day-night = 401 deg
H' (km)

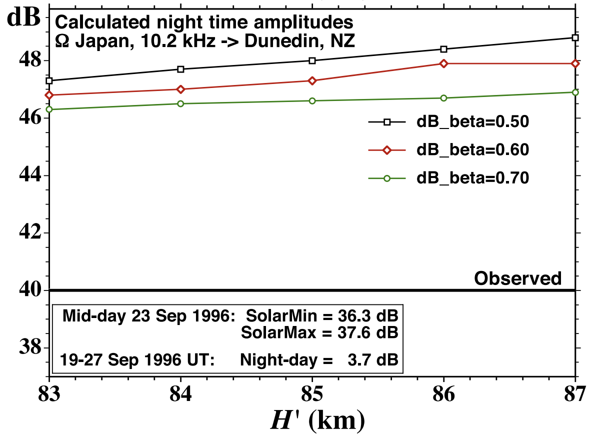
dB
Calculated night time amplitudes
Ω Japan, 10.2 kHz -> Dunedin, NZ
dB_beta=0.50
dB_beta=0.60
dB_beta=0.70
Observed
Mid-day 23 Sep 1996: SolarMin = 36.3 dB
SolarMax = 37.6 dB
19-27 Sep 1996 UT: Night-day = 3.7 dB
H' (km)

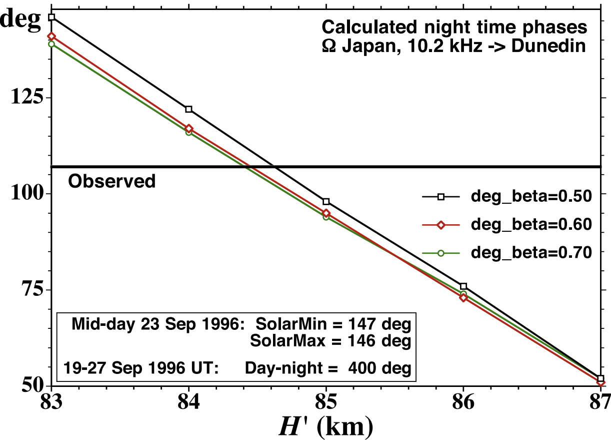
deg
Calculated night time phases
Ω Japan, 10.2 kHz -> Dunedin
Observed
deg_beta=0.50
deg_beta=0.60
deg_beta=0.70
Mid-day 23 Sep 1996: SolarMin = 147 deg
SolarMax = 146 deg
19-27 Sep 1996 UT: Day-night = 400 deg
H' (km)

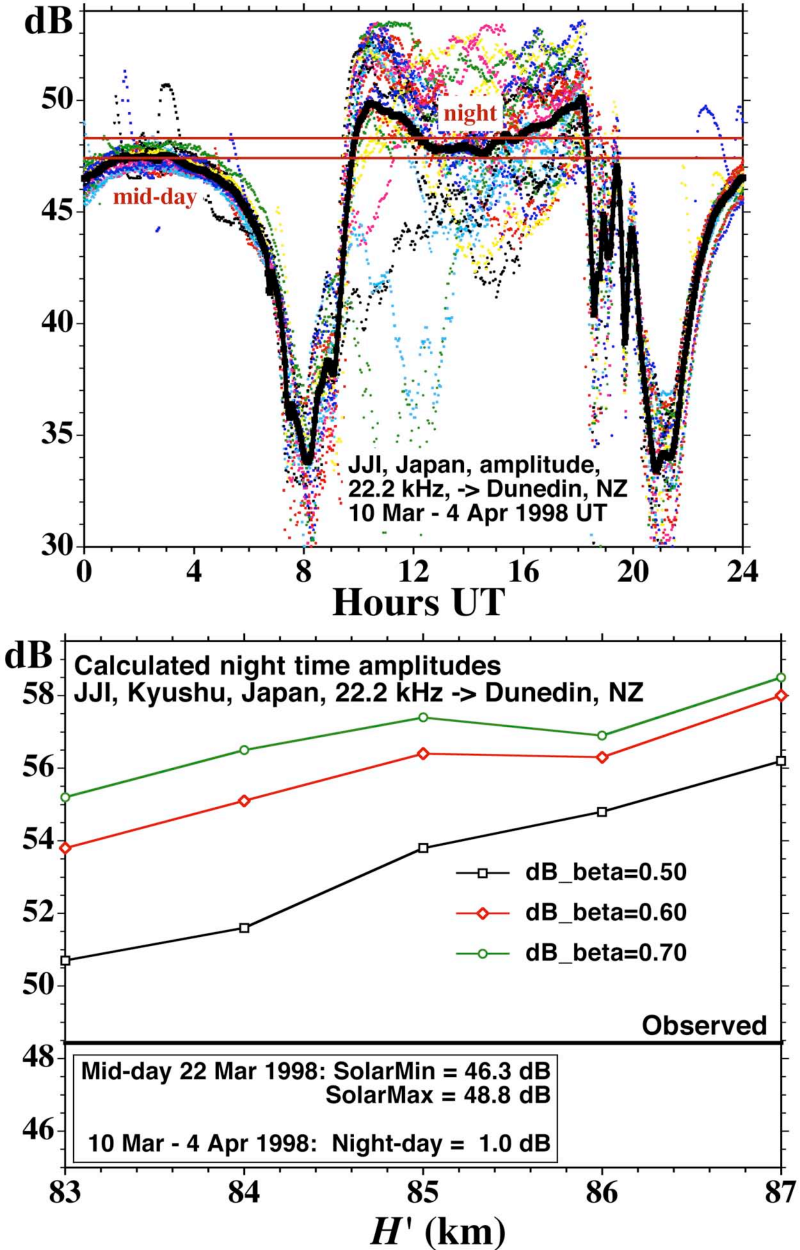
dB
50
45
40
35
30
night
mid-day
JJI, Japan, amplitude,
22.2 kHz, -> Dunedin, NZ
10 Mar - 4 Apr 1998 UT
0
4
8
12
16
20
24
Hours UT
dB
Calculated night time amplitudes
JJI, Kyushu, Japan, 22.2 kHz -> Dunedin, NZ
58
56
54
52
50
48
46
dB_beta=0.50
dB_beta=0.60
dB_beta=0.70
Observed
Mid-day 22 Mar 1998: SolarMin = 46.3 dB
SolarMax = 48.8 dB
10 Mar - 4 Apr 1998: Night-day = 1.0 dB
83
84
85
86
87
H' (km)

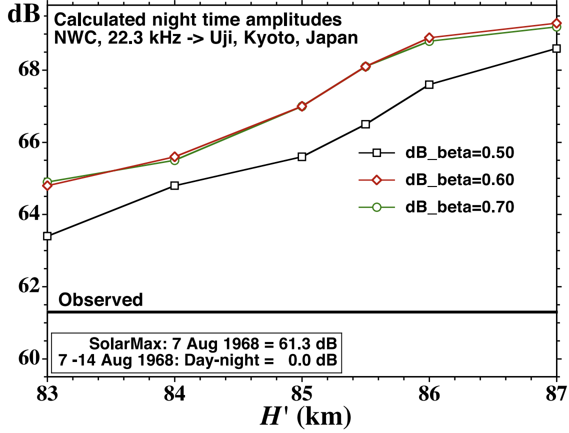
dB
Calculated night time amplitudes
NWC, 22.3 kHz -> Uji, Kyoto, Japan
68
66
64
62
60
dB_beta=0.50
dB_beta=0.60
dB_beta=0.70
Observed
SolarMax: 7 Aug 1968 = 61.3 dB
7 -14 Aug 1968: Day-night = 0.0 dB
83
84
85
86
87
H' (km)

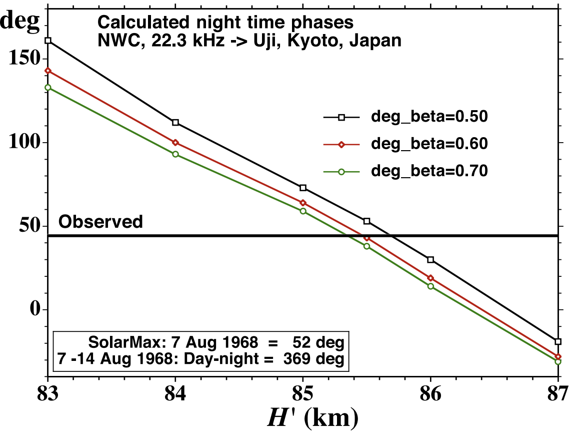
deg
Calculated night time phases
NWC, 22.3 kHz -> Uji, Kyoto, Japan
150
100
50
0
deg_beta=0.50
deg_beta=0.60
deg_beta=0.70
Observed
SolarMax: 7 Aug 1968 = 52 deg
7 -14 Aug 1968: Day-night = 369 deg
83
84
85
86
87
H' (km)

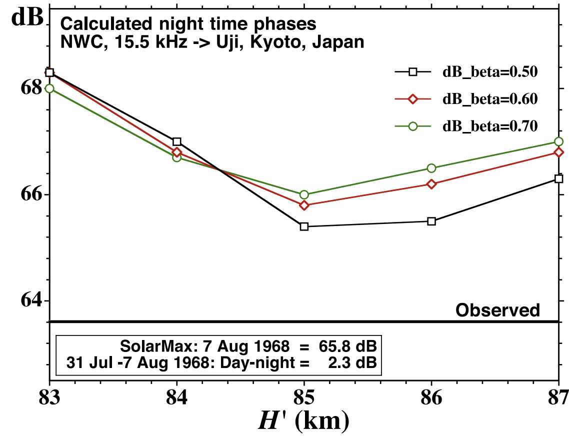
dB
Calculated night time phases
NWC, 15.5 kHz -> Uji, Kyoto, Japan
68
66
64
dB_beta=0.50
dB_beta=0.60
dB_beta=0.70
Observed
SolarMax: 7 Aug 1968 = 65.8 dB
31 Jul -7 Aug 1968: Day-night = 2.3 dB
83
84
85
86
87
H' (km)

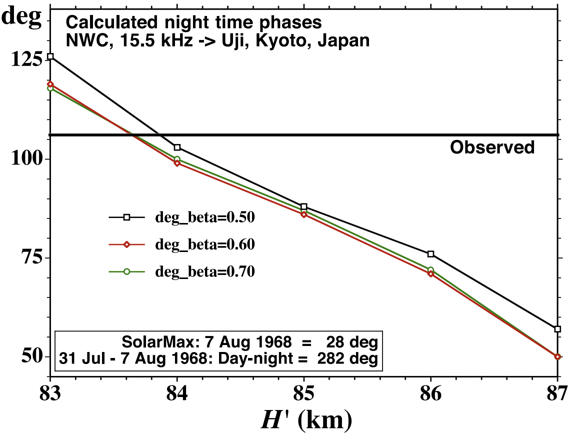
deg
Calculated night time phases
NWC, 15.5 kHz -> Uji, Kyoto, Japan
125
100
75
50
Observed
deg_beta=0.50
deg_beta=0.60
deg_beta=0.70
SolarMax: 7 Aug 1968 = 28 deg
31 Jul - 7 Aug 1968: Day-night = 282 deg
83
84
85
86
87
H' (km)

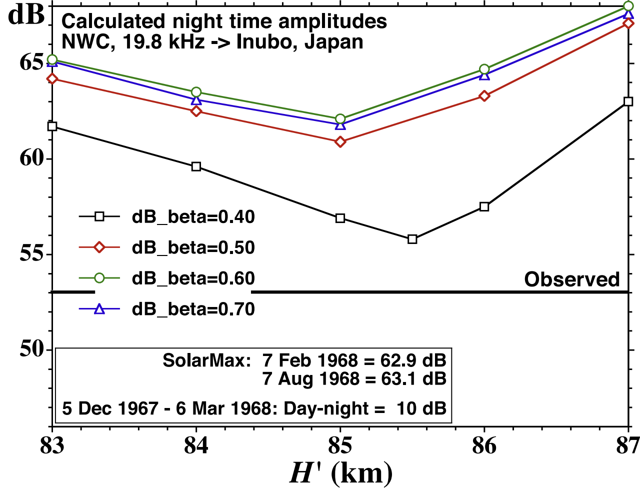
dB
Calculated night time amplitudes
NWC, 19.8 kHz -> Inubo, Japan
65
60
55
50
dB_beta=0.40
dB_beta=0.50
dB_beta=0.60
dB_beta=0.70
Observed
SolarMax: 7 Feb 1968 = 62.9 dB
7 Aug 1968 = 63.1 dB
5 Dec 1967 - 6 Mar 1968: Day-night = 10 dB
83
84
85
86
87
H' (km)

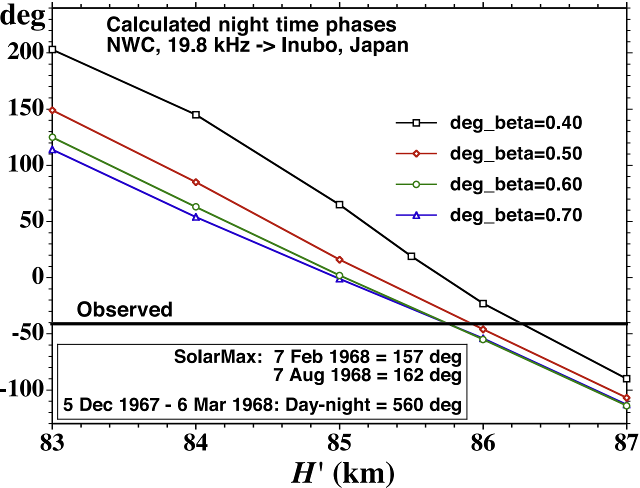
deg
Calculated night time phases
NWC, 19.8 kHz -> Inubo, Japan
200
150
100
50
0
-50
-100
deg_beta=0.40
deg_beta=0.50
deg_beta=0.60
deg_beta=0.70
Observed
SolarMax: 7 Feb 1968 = 157 deg
7 Aug 1968 = 162 deg
5 Dec 1967 - 6 Mar 1968: Day-night = 560 deg
83
84
85
86
87
H' (km)

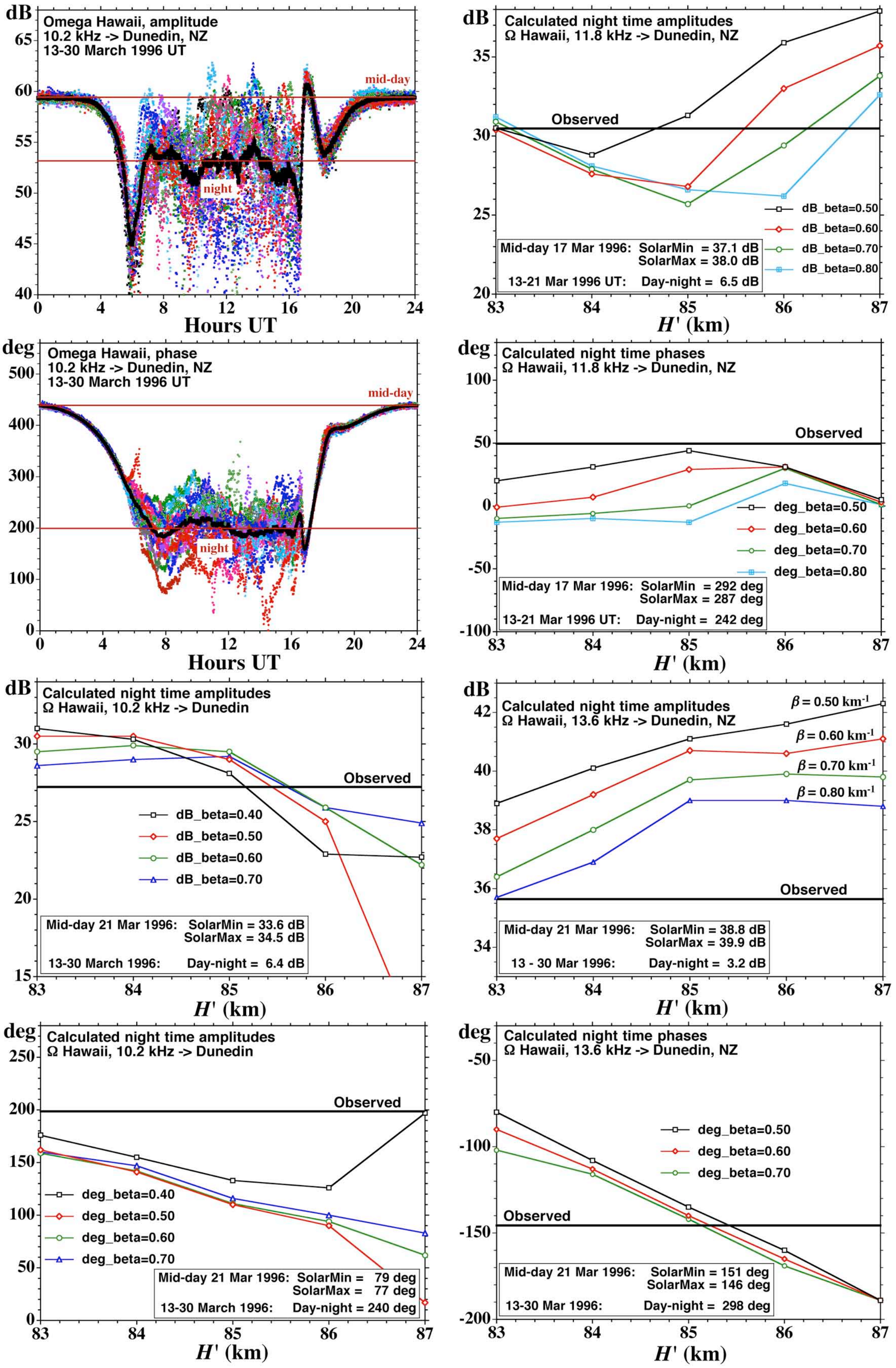

Omega Hawaii, amplitude
10.2 kHz -> Dunedin, NZ
13-30 March 1996 UT
mid-day
night
dB
Hours UT
Calculated night time amplitudes
Ω Hawaii, 11.8 kHz -> Dunedin, NZ
Observed
dB_beta=0.50
dB_beta=0.60
dB_beta=0.70
dB_beta=0.80
Mid-day 17 Mar 1996: SolarMin = 37.1 dB
SolarMax = 38.0 dB
13-21 Mar 1996 UT: Day-night = 6.5 dB
H' (km)
Omega Hawaii, phase
10.2 kHz -> Dunedin, NZ
13-30 March 1996 UT
mid-day
night
deg
Hours UT
Calculated night time phases
Ω Hawaii, 11.8 kHz -> Dunedin, NZ
Observed
deg_beta=0.50
deg_beta=0.60
deg_beta=0.70
deg_beta=0.80
Mid-day 17 Mar 1996: SolarMin = 292 deg
SolarMax = 287 deg
13-21 Mar 1996 UT: Day-night = 242 deg
H' (km)
Calculated night time amplitudes
Ω Hawaii, 10.2 kHz -> Dunedin
Observed
dB_beta=0.40
dB_beta=0.50
dB_beta=0.60
dB_beta=0.70
Mid-day 21 Mar 1996: SolarMin = 33.6 dB
SolarMax = 34.5 dB
13-30 March 1996: Day-night = 6.4 dB
H' (km)
Calculated night time amplitudes
Ω Hawaii, 13.6 kHz -> Dunedin, NZ
β = 0.50 km⁻¹
β = 0.60 km⁻¹
β = 0.70 km⁻¹
β = 0.80 km⁻¹
Observed
Mid-day 21 Mar 1996: SolarMin = 38.8 dB
SolarMax = 39.9 dB
13 - 30 Mar 1996: Day-night = 3.2 dB
H' (km)
Calculated night time amplitudes
Ω Hawaii, 10.2 kHz -> Dunedin
Observed
deg_beta=0.40
deg_beta=0.50
deg_beta=0.60
deg_beta=0.70
Mid-day 21 Mar 1996: SolarMin = 79 deg
SolarMax = 77 deg
13-30 March 1996: Day-night = 240 deg
H' (km)
Calculated night time phases
Ω Hawaii, 13.6 kHz -> Dunedin, NZ
deg_beta=0.50
deg_beta=0.60
deg_beta=0.70
Observed
Mid-day 21 Mar 1996: SolarMin = 151 deg
SolarMax = 146 deg
13-30 Mar 1996: Day-night = 298 deg
H' (km)

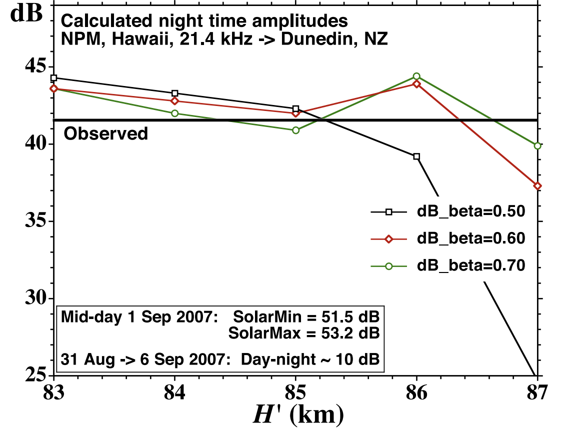
Calculated night time amplitudes
NPM, Hawaii, 21.4 kHz -> Dunedin, NZ
dB
45
40
35
30
25
Observed
dB_beta=0.50
dB_beta=0.60
dB_beta=0.70
Mid-day 1 Sep 2007: SolarMin = 51.5 dB
SolarMax = 53.2 dB
31 Aug -> 6 Sep 2007: Day-night ~ 10 dB
83
84
85
86
87
H' (km)

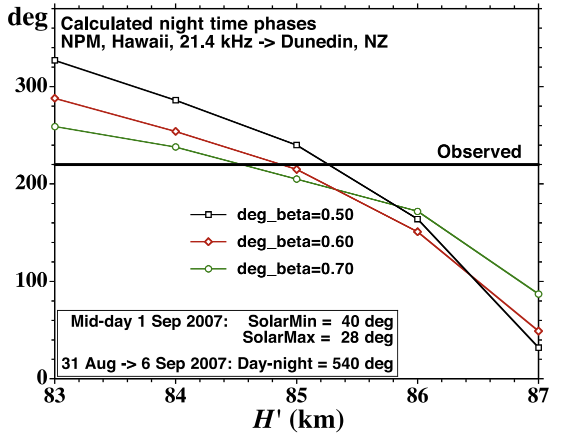
Calculated night time phases
NPM, Hawaii, 21.4 kHz -> Dunedin, NZ
deg
300
200
100
0
Observed
deg_beta=0.50
deg_beta=0.60
deg_beta=0.70
Mid-day 1 Sep 2007: SolarMin = 40 deg
SolarMax = 28 deg
31 Aug -> 6 Sep 2007: Day-night = 540 deg
83
84
85
86
87
H' (km)

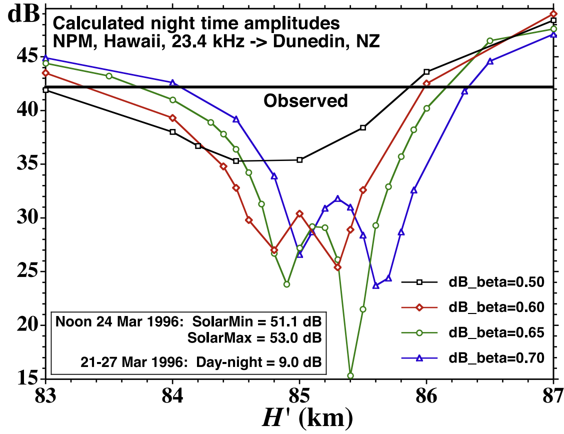
Calculated night time amplitudes
NPM, Hawaii, 23.4 kHz -> Dunedin, NZ
dB
45
40
35
30
25
20
15
Observed
dB_beta=0.50
dB_beta=0.60
dB_beta=0.65
dB_beta=0.70
Noon 24 Mar 1996: SolarMin = 51.1 dB
SolarMax = 53.0 dB
21-27 Mar 1996: Day-night = 9.0 dB
83
84
85
86
87
H' (km)

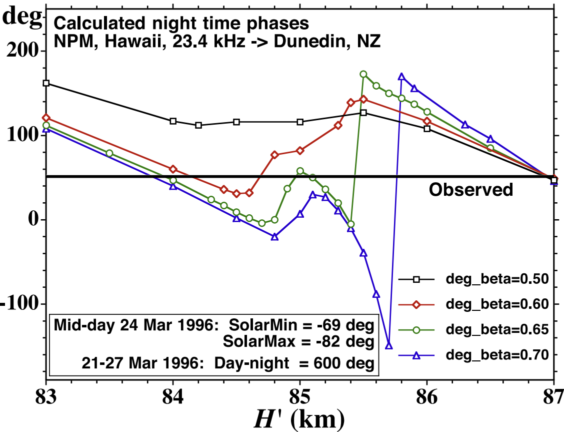
Calculated night time phases
NPM, Hawaii, 23.4 kHz -> Dunedin, NZ
deg
200
100
0
-100
Observed
deg_beta=0.50
deg_beta=0.60
deg_beta=0.65
deg_beta=0.70
Mid-day 24 Mar 1996: SolarMin = -69 deg
SolarMax = -82 deg
21-27 Mar 1996: Day-night = 600 deg
83
84
85
86
87
H' (km)